engineering proceedings

MDPI

Proceeding Paper

Strong Coupling Dynamics of a Quantum Emitter Near a Bi_2Te_3 Nanoparticle †

Ioannis Thanopulos [1,*], Vassilios Yannopapas [2] and Emmanuel Paspalakis [1]

[1] Materials Science Department, School of Natural Sciences, University of Patras, 265 04 Patras, Greece; email1@email.com
[2] Department of Physics, National Technical University of Athens, 157 80 Athens, Greece; email2@email.com
* Correspondence: ithano@upatras.gr
† Presented at the 4th International Electronic Conference on Applied Sciences, 27 October–10 November 2023; Available online: https://asec2023.sciforum.net/.

Abstract: We study the spontaneous emission (SPEM) of a quantum emitter (QE) near a topological insulator Bi_2Te_3 spherical nanoparticle (SNP). We use the electromagnetic Green's tensor method for calculating the Purcell factor for the QE near the SNP using parameters from experiment for describing the topological insulator optical properties. We find exceptional Purcell factors of the QE up to 10^{10} at distances between the QE and the SNP as large as half its radius in the terahertz regime. We study the dynamics of the SPEM of a QE with transition frequency in the terahertz and vacuum decay rates, which affects inversely proportional the interaction strength between the QE and the SNP, in the ns to μs range. For short vacuum decay times, we observe non-Markovian SPEM dynamics, which corresponds perfectly to values of standard measures of non-Markovianity and indicates possibly considerable dynamical quantum speedup. The dynamics turns progressively Markovian as the vacuum decay time increases, while then the non-Markovianity measures are nullified and the quantum speedup vanishes.

Keywords: spontaneous emission; topological insulator; Bi_2Te_3; two-level quantum system; purcell effect; strong coupling; non-markovianity measure; quantum speed limit

Citation: Thanopulos, I.; Yannopapas, V.; Paspalakis, E. Strong Coupling Dynamics of a Quantum Emitter Near a Bi_2Te_3 Nanoparticle. *Eng. Proc.* **2023**, *52*, 0. https://doi.org/

Academic Editor: Firstname Lastname

Published:

1. Introduction

In the last decade, the strong coupling of quantum emitters (QEs) with photonic microstructures and nanostructures pushes the boundaries of cavity quantum electrodynamics in new regimes and may lead to numerous important phenomena in nanophotonics and applications in quantum technologies [1]. A basic phenomenon under strong coupling of a QE with its nanophotonic surroundings is the exchange of energy between the QE and the photonic nanostructure in a coherent manner, leading to non-Markovian and reversible spontaneous emission (SPEM) dynamics of a QE. This phenomenon has been predicted when a QE is coupled to various nanophotonic platforms, including plasmonic nanostructures [2], epsilon-and-mu-near-zero media [3], two-dimensional semiconductors [4], graphene nanostructures [5], and ferromagnetic or ferrimagnetic nanoparticles [6]. Another class of photonic structures that induce strong light-matter interaction with QEs emerges through the merger of quantum optics with topological photonics [7], and is realized by coupling QEs with topological photonic structures, like topological one-dimensional waveguides [8], three-dimensional photonic Weyl environments [9], topological photonic crystals [10], and a plasmonic nanoantenna, for on-resonance operation, embedded in a topological photonic structure designed for this purpose [11].

Here, we explore nanophotonics on a Be_2Te_3 platform, in order to obtain strong coupling between light and matter, resulting into non-Markovian SPEM between a QE and a spherical nanoparticle (SNP) made of a topological insulator [12]. Recently, the interaction

of light with topological insulator nanoparticles (TINPs) has shown interesting optical properties [13–16].

2. Theory

In this work we investigate the non-Markovian dynamics of an one-photon SPEM of a QE next to a Bi_2Te_3 TINP of radius R. A SNP-centered coordinate system is in use, as shown in the left panel of Figure 1, where a QE placed at $\tilde{\mathbf{r}}_{QE} = (0, 0, R + D)$ is shown.

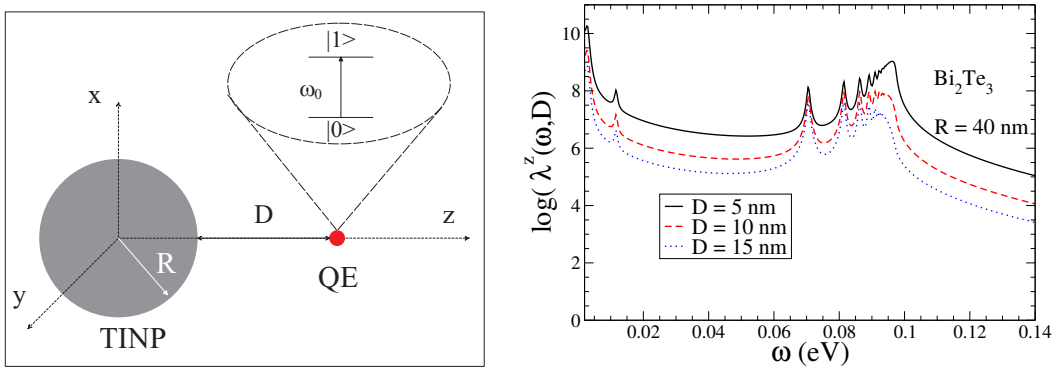

Figure 1. (color online) Left: Schematic depiction of a topological insulator nanoparticle (TINP), a Bi_2Te_3 sphere of radius R, in proximity to a two-level quantum emitter (QE), as in this work. Right: Purcell enhancement factor of a QE with a transition dipole moment along the z direction close to a Bi_2Te_3 SNP of $R = 40$ nm for several D.

The system-state reads (in this work we use $\hbar = 1$)

$$|\Psi(t)\rangle = c_1(t)e^{-i\omega_0 t}|1;0_\omega\rangle + \int d\vec{r} \int d\omega\, c(\vec{r},\omega,t)e^{-i\omega t}|0;1_{\vec{r},\omega}\rangle\,. \tag{1}$$

In Equation (1), $|n;a\rangle = |n\rangle \otimes |a\rangle$, stands for the states of the two-level quantum system, where $|n\rangle$ $(n = 0, 1)$, and $|a\rangle$ stands for the states of the modified modes of the electromagnetic continuum due to the proximity to the TINP, with the vacuum given by $|0_\omega\rangle$ and the one-photon state by $|1_{\vec{r},\omega}\rangle$. The equation for $c_1(t)$ reads [2]

$$\dot{c}_1(t) = i\int_0^t K(t-t')c_1(t')dt', \;\; K(t-t') = ie^{i\omega_0(t-t')}\int_0^\infty J(\omega)e^{-i\omega(t-t')}d\omega\,, \tag{2}$$

with $J(\omega) = \Gamma_0(\omega_0)\lambda^z(\omega, D)/2\pi$, and $\Gamma_0(\omega_0)$ being the vacuum decay width of a QE with resonance frequency ω_0 in free-space; also, $\lambda^z(\omega, D)$ denotes the Purcell factor of the QE with a z-oriented (radial) transition dipole moment located at distance D from the TINP surface. The probability amplitude dynamics is computed using the effective mode differential equation (EMDE) methodology [2].

The influence of the altered continuum of electromagnetic modes due to the proxiity to the TINP to the QE, located at distance D from the surface of the SNP of radius R is quantified by calculating the radial Purcell factor, $\lambda^z(\omega, D) = \frac{\Gamma^z(\omega)}{\Gamma_0(\omega)}$, using a numerical electromagnetic Green's tensor method [2,17]. The absorption cross-section $\sigma_{abs}(\omega)$ given by [13]

$$\sigma_{abs}(\omega) = 4\pi R\frac{\omega}{c}\mathrm{Im}\left[\frac{\epsilon(\omega)+\delta_R-1}{\epsilon(\omega)+\delta_R+2}\right] \tag{3}$$

is determined by the electric field boundary conditions, with $\epsilon(\omega)$ being the dielectric function of Bi_2Te_3. In Equation (3), δ_R denotes the term related to light-induced transitions between the delocalized topologically protected states. Here we consider $\delta_R = 0$; then Equation (3) describes practically the case of a dielectric sphere in an uniform field.

In Equations (3), the dielectric function $\epsilon(\omega)$ is given by [13] $\epsilon(\omega) = \sum_{i=a,\beta,f} \frac{\omega_{pi}^2}{\omega_{0i}^2 - \omega^2 - i\gamma_i\omega}$ including a and β transverse phonon contributions [18]; it also includes contributions from free charge carriers (with index f) due to defects in the bulk, while the parameters are obtained from fitting to bulk experimental data [14]: $\omega_{pa} = 21$ THz, $\omega_{p\beta} = 4$ THz, $\omega_{pf} = 11$ THz, $\omega_{0a} = 1.56$ THz, $\omega_{0\beta} = 2.85$ THz, $\omega_{0f} = 0$ THz, $\gamma_a = 0.18$ THz, $\gamma_\beta = 0.2$ THz, and $\gamma_f = 0.24$ THz. Note that in this work, since we operate in the QE near field regime, the distance, D, is much smaller than the wavelength of the QE SPEM photon, λ; therefore, the use of the electrostatic approximation is justified.

3. Results and Discussion

We investigate the SPEM dynamics of a QE with a z-oriented transition dipole moment in proximity to a Bi_2Te_3 SNP with $R = 40$ nm, when $\delta_R = 0$. In the right panel of Figure 1 we show the Purcell enhancement factor of such a QE for several D.

We focus on the dynamics of the SPEM in case of a QE with $\omega_0 = 0.070457$ eV $=$ 17.036 THz and transition dipole moment along the z-axis, when the QE is located at $D = 20$ nm from the surface of a $R = 40$ nm Bi_2Te_3 SNP. We find, that the decay of the QE population occurs in an oscillatory way, with decreasing frequency of oscillation, as the vacuum decay time becomes longer; this fact is clearly indicating the transition from non-Markovian to Markovian dynamics.

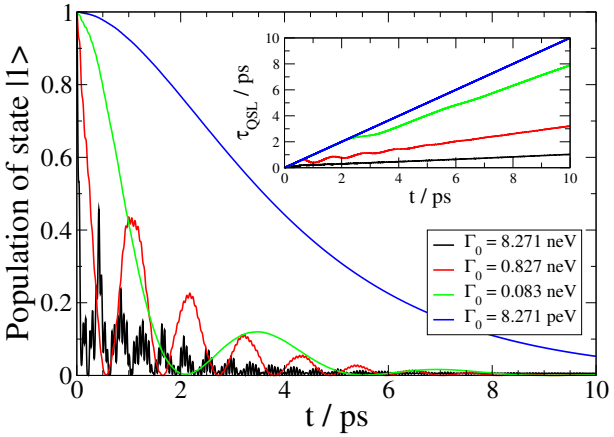

Figure 2. (color online) SPEM dynamics for a QE with $\omega_0 = 0.070457$ eV $= 17.03643$ THz and transition dipole moment along the z-axis located at $D = 20$ nm from a Bi_2Te_3 SNP with radius $R = 40$ nm and the QSL of the corresponding dynamics (inset).

In the inset of Figure 2 we further show the quantum speed limit (QSL) τ_{QSL} for the SPEM dynamics. The minimal evolution of an open quantum system [21] is bounded by the QSL, and it is related to the non-Markovianity of the dynamics by [22]

$$\tau_{QSL} = \frac{t}{2\frac{\tilde{N}(t)}{1-|c_1(t)|^2}+1}, \quad \tilde{N}(t) = 0.5\int_0^t |\partial_{t'}[c_1(t')c_1^*(t')]|dt' + [c_1(t')c_1^*(t')] - 1\,, \qquad (4)$$

with t denoting the actual driving time of the open system. Thus, when $\tilde{N} = 0$, Equation (4) implies that the QSL is equal to t; otherwise, QSL always has a smaller value that t. Therefore, one concludes that by exploitation of the open system non-Markovianity, its actual dynamics can be accelerated with respect to the corresponding Markovian dynamics.

The above observations regarding the SPEM dynamics, which is shown in the main panel of Figure 2, can be also drawn through the QSL of the corresponding dynamics, shown in the inset of Figure 2. We observe that the QSL curves tend to align with the (conceivable) graph diagonal as the vacuum decay width decreases; the QSL curve, for the smallest vacuum decay width, actually fully overlaps with the diagonal, as expected from the corresponding Markovian population dynamics.

We also study the non-Markovian features of the SPEM dynamics by applying three measures of non-Makovianity in order to characterize the coupling between the QE and the continuum of electromagnetic modes as affected by the TINP: The Breuer, Laine, Pillo (BLP) measure, $\mathcal{N}$, defined in Ref. [23], based on the quantum system - environment information flow, which quantifies the non-Markovianity of the process by using the two-state trace distance, and the two Rivas, Huelga, Plenio (RHP) measures, $\mathcal{I}^E$ and $\mathcal{I}$, defined in Ref. [24], that quantify the non-Markovian features of the dynamics of entanglement by applying local completely positive maps that preserve the trace. Note, when applied to a two-state QE interacting to photonic environments with couplings that depend on frequency, the $\mathcal{N}$, $\mathcal{I}^E$ and $\mathcal{I}$ measures are equivalent [25].

For computing the non-Markovianity measure values, we make use of the following quantities

$$\gamma(t) = -2\Re\left(\frac{\dot{c}_1(t)}{c_1(t)}\right) = -\frac{2}{|c_1(t)|}\frac{d}{dt}|c_1(t)|, \text{ and } F(t) = \frac{a^2 e^{-\frac{3}{2}\Gamma(t)} + \frac{1}{2}|b|^2 e^{-\frac{1}{2}\Gamma(t)}}{\sqrt{a^2 e^{-\Gamma(t)} + |b|^2}}, \quad (5)$$

with $\Gamma(t) = \int_0^t dt' \gamma(t')$, $a = \langle 1|\rho_1(0)|1\rangle - \langle 1|\rho_2(0)|1\rangle$ being the population difference, and $b = \langle 1|\rho_1(0)|0\rangle - \langle 1|\rho_2(0)|0\rangle$ being the coherence difference between the two arbitrary initial states. Then, the BLP measure [23] reads:

$$\mathcal{N} = -\max_{a,b} \int_{\gamma(t)<0} \gamma(t) F(t) dt\,. \quad (6)$$

Also, the RHP measures [24] read:

$$\mathcal{I}^{(E)} = -\int_{\gamma(t)<0} \gamma(t) e^{-\frac{1}{2}\Gamma(t)} dt, \quad \mathcal{I} = -\int_{\gamma(t)<0} \gamma(t) dt\,. \quad (7)$$

Table 1. Value of Non-Markovianity measures [23,24] for several vacuum decay width in case of a QE with transition energy ω_0 at $D = 20$ nm from a Bi_2Te_3 SNP of radius $R = 40$ nm.

	$\omega_0 = 0.070457$ eV			
Γ_0 / neV	8.271	0.827	0.083	0.008
$\mathcal{N}$	13.41	2.91	0.41	0
$\mathcal{I}^E$	26.82	5.83	0.82	0
$\mathcal{I}$	312.26	121.20	8.95	0

Lastly, in Table 1 we show the $\mathcal{N}$, $\mathcal{I}^E$, and $\mathcal{I}$ non-Markovianity measures for various Γ_0 in case of a QE with transition energy $\omega_0 = 0.070457$ eV $= 17.03643$ THz at $D = 20$ nm from a $R = 40$ nm Bi_2Te_3 SNP. The values decrease as the population dynamics oscillation frequency decreases, since in all three cases, by definition, only the $\gamma(t) < 0$ part of the dynamics contributes to the measure value. Note, that each measure value is not normalized; thus, no comparison between the measures is possible.

4. Conclusions

In this work we study the light-matter coupling conditions of a QE near a SNP of Bi_2Te_3, a topological insulator material, without inclusion of the topologically protected delocalized surface states. By using first-principle electromagnetic methods, we compute the Purcell factor of a QE, with radial transition dipole moment with respect to a $R = 40$ nm radius SNP, for various distance values between the QE and the surface of the SNP. We use experimental parameters for describing the optical properties of the Bi_2Te_3 material. We find exceptionally high enhancement factors, up to 10^{10}, while the enhancement factors remain large, above 10^5, within the whole frequency range up to 0.14 eV.

More specifically, we investigate the SPEM dynamics of the QE near a Bi_2Te_3 SNP for vacuum decay in the nanoseconds to milliseconds time range. For large vacuum decay width values, we observe that the dynamics of the SPEM is distinctively non-Markovian. Moreover, when the QE ω_0 is resonant to an isolated polariton of the Bi_2Te_3 SNP, the dynamics of the SPEM features population transfer in a complete oscillatory manner (Rabi oscillations) from the QE into the continuum of electromagnetic modes as altered by the TINP nanosphere and back. As the vacuum decay width decreases, the dynamics of the SPEM turn to Markovian, with the population of the QE waning out in the continuum of electromagnetic modes practically in exponential way.

We also calculate the BLP and RHP non-Markovianity measure values for the cases studied. The measure values decrease as the underlying dynamics turn to Markovian. Additionally, the QSL of the dynamics of the SPEM is computed; we find that when the light-matter interaction is strong, resulting into non-Markovian behavior, the dynamics can be significantly accelerated.

In conclusion, we have shown that a Bi_2Te_3 SNP can provide the conditions for achieving strong light-matter coupling at the nanoscale. Moreover, we have considered QEs with realistic vacuum decay times for various systems at the nanoscale, thus rendering our results particularly interesting and promising towards quantum technologies development.

Author Contributions: Conceptualization, E.P.; methodology, I.T., V.Y. and E.P.; software, V.Y.; visualization, I.T.; validation, I.T., V.Y. and E.P.; investigation, I.T., V.Y. and E.P.; writing—original draft preparation, I.T., V.Y. and E.P.; writing—review and editing, I.T., V.Y. and E.P.; supervision, I.T., V.Y. and E.P. All authors have read and agreed to the published version of the manuscript.

Funding:

Institutional Review Board Statement:

Informed Consent Statement:

Data Availability Statement: The data presented in this study are available upon reasonable request from the corresponding author.

Acknowledgments: We gratefully acknowledge help and stimulating discussions with A. G. Vanakaras. The work of I.T. was funded by an Empirikion Foundation research grant.

Conflicts of Interest: The authors declare no conflict of interest.

Abbreviations

The following abbreviations are used in this manuscript:

QE	Quantum Emitter
SPEM	Spontaneous Emission
TINP	Topological Insulator Nanoparticle
SNP	Spherical Nanoparticle
BLP	Brueuer, Laine, Pillo
RHP	Rivas, Huelga, Plenio
QSL	Quantum Speed Limit

References

1. Zhang, Q.; Gong, Q.-H.; Gu, Y, Enhanced Photon-Emitter Coupling in Micro/Nano Photonic Structures. *IEEE J. Select. Top. Quant. Electron.* **2021**, *27*, 6700310.
2. Thanopulos, I.; Yannopapas, V.; Paspalakis, E. Non-Markovian dynamics in plasmon-induced spontaneous emission interference. *Phys. Rev. B* **2017**, *95*, 075412.
3. Liberal, I.; Engheta, N. Zero-index structures as an alternative platform for quantum optics. *Proc. Natl. Acad. Sci. USA* **2017**, *114*, 822.
4. Thanopulos, I.; Karanikolas, V.; Paspalakis, E. Strong interaction of quantum emitters with a WS_2 layer enhanced by a gold substrate. *IEEE J. Select. Top. Quant. Electron.* **2021**, *27*, 6700108.
5. Thanopulos, I.; Karanikolas, V.; Paspalakis, E. Spontaneous emission of a quantum emitter near a graphene nanodisk under strong light-matter coupling. *Phys. Rev. A* **2022**, *106*, 013718.

6. Neuman, T.; Wang, D.S.; Narang, P. Nanomagnonic Cavities for Strong Spin-Magnon Coupling and Magnon-Mediated Spin-Spin Interactions. *Phys. Rev. Lett.* **2020**, *125*, 247702.
7. Ozawa, T.; Price, H.M.; Amo, A.; Goldman, N.; Hafezi, M.; Lu, L.; Rechtsman, M.C.; Schuster, D.; Simon, J.; Zilberberg, O.; et al. Topological photonics. *Rev. Mod. Phys.* **2019**, *91*, 015006.
8. Bello, M.; Platero, G.; Cirac, J.I.; González-Tudela, A. Unconventional quantum optics in topological waveguide QED. *Sci. Adv.* **2019**, *5*, eaaw0297.
9. García-Elcano, I.; González-Tudela, A.; Bravo-Abad, J. Tunable and Robust Long-Range Coherent Interactions between Quantum Emitters Mediated by Weyl Bound States. *Phys. Rev. Lett.* **2020**, *125*, 163602.
10. Barik, S.; Karasahin, A.; Flower, C.; Cai, T.; Miyake, H.; DeGottardi, W.; Hafezi, M.; Waks, E. A topological quantum optics interface. *Science* **2018**, *359*, 666.
11. Qian, Z.-Y.; Li, Z.-C.; Hao, H.; Shan, L.-X.; Zhang, Q.; Dong, J.-W.; Gong, Q.-H.; Gu, Y. Absorption reduction of large purcell enhancement enabled by topological state-led mode coupling. *Phys. Rev. Lett.* **2021**, *126*, 023901.
12. Hasan, M.Z.; Kane, C.L. Topological Insulators. *Rev. Mod. Phys.* **2010**, *82*, 3045.
13. Siroki, G.; Lee, D.K.K.; Hayes, P.D.; Giannini, V. Single-electron induced surface plasmons on a topological nanoparticle. *Nat. Commun.* **2016**, *7*, 12375.
14. Rider, M.S.; Sokolikova, M.; Hanham, S.M.; Navarro-Cía, M.; Haynes, P.D.; Lee, D.K.K.; Daniele, M.; Cestelli Guildi, M.; Mattevi, C.; Lupi, S.; et al. Experimental signature of a topological quantum dot. *Nanoscale* **2020**, *12*, 22817.
15. Chatzidakis, G.D.; Yannopapas, V. Strong electromagnetic coupling in dimers of topological-insulator nanoparticles and quantum emitters. *Phys. Rev. B* **2020**, *101*, 165410.
16. Karaoulanis, D.; Paspalakis, E.; Yannopapas, V. Quantum interference near bismuth-chalcogenide microstructures. *J. Opt. Soc. Am. B* **2021**, *38*, 3301.
17. Yannopapas, V.; Vitanov, N.V. Electromagnetic Green's tensor and local density of states calculations for collections of spherical electromagnetic scatterers. *Phys. Rev. B* **2007**, *75*, 115124.
18. Butch, N.P.; Kirschenbaum, K.; Syers, P.; Sushkov, A.B.; Jenkins, G.S.; Drew, H.D.; Paglione, J. Strong surface scattering in ultra-high mobility Bi_2Se_3 topological insulator crystalls. *Phys. Rev. B* **2010**, *81*, 241301(R).
19. Thanopulos, I.; Yannopapas, V.; Paspalakis, E. Topological insulator nanoparticle for strong light-matter interaction in the terahertz. *Opt. Lett.* **2022**, *49*, 5240.
20. Shi, T.; Wu, Y.-H.; González-Tudela, A.; Cirac, J.I. Bound States in Boson Impurity Models. *Phys. Rev. X* **2016**, *6*, 021027.
21. Deffner, S.; Lutz, E. Quantum Speed Limit for Non-Markovian Dynamics. *Phys. Rev. Lett.* **2013**, *111*, 010402.
22. Xu, Z.-Y.; Luo, S.; Yang, W.L.; Liu, C.; Zhu, S. Quantum speedup in a memory environment. *Phys. Rev. A* **2014**, *89*, 012307.
23. Breuer, H.-P.; Laine, E.-M.; Piilo, J. Measure for the degree of non-Markovian behaviour of quantum processes in open systems. *Phys. Rev. Lett.* **2009**, *103*, 210401.
24. Rivas, A.; Huelga, S.F.; Plenio, M.B. Entanglement and Non-Markovianity of quantum evolutions. *Phys. Rev. Lett.* **2010**, *105*, 050403.
25. Zeng, H.-S.; Tang, N.; Zheng, Y.-P.; Wang, G.-Y. Equivalence of the measures of Non-Markovianity for open two-level systems. *Phys. Rev. A* **2011**, *84*, 032118.